NASA CR

SEMI-ANNUAL PROGRESS REPORT, October 1993 - March 1994

NASA GRANT NUMBER NCC 2-834

Modification of ACSYNT Aircraft Computer Program for Preliminary Design

Daniel J. Biezad
Ruben Rojos-Oviedo

Graduate Assistant: Angelen Ngan

NASA Ames Research Center
Aircraft Guidance and Navigation Branch
Moffett Field, CA 94035-1000

31 March 1994

ABSTRACT

The period between October, 1993, and April, 1994, was spent preparing a paper for the 7th Biennial AIAA Flight Test Conference to be held this coming June in Colorado Springs, Colorado. The paper abstract is attached and adequately summarizes the work accomplished to date.

The NASA Technical Officer for this grant is Paul Gelhausen, NASA Ames Research Center, Moffett Field, CA.

AIAA 94-2135

INCORPORATING AGILITY FLIGHT TEST METRICS CONCURRENTLY INTO THE AIRCRAFT PRELIMINARY DESIGN PROCESS

B. Bauer, D. Biezad, R. Rojas-Oviedo, A. Ngan, and D. Sandlin
Aeronautical Engineering Department
Cal Poly State University
San Luis Obispo, CA 93407

7th Biennial AIAA Flight Test Conference

June 20-23, 1994 / Colorado Springs, CO

INCORPORATING AGILITY FLIGHT TEST METRICS CONCURRENTLY INTO THE AIRCRAFT PRELIMINARY DESIGN PROCESS

B. Bauer, D. Biezad, R. Rojas-Oviedo, A. Ngan, and D. Sandlin
Aeronautical Engineering Department
Cal Poly State University
San Luis Obispo, CA 93407

Abstract

This paper presents the development of a computer simulation of agility flight test techniques. Its purpose is to evaluate the agility of aircraft configurations early in the preliminary design phase. The simulation module is integrated into the NASA Ames aircraft synthesis design code. Trade studies using the agility module embedded within the design code to simulate the combat cycle time agility metric are illustrated using a Northrop F-20 aircraft model. Results show that the agility module is effective in analyzing the influence of common parameters such as thrust-to-weight ratio and wing loading on agility criteria. The module can also compare the agility potential between different configurations and has the capability to optimize agility performance early in the design process.

Nomenclature

a_F	Acceleration normal to flight path
a_{cent}	Centripetal acceleration (reaction)
a_x	Acceleration along flight path direction
n	Load factor
p	Roll rate
Ps	Specific excess power
p_{ss}	Steady state roll rate
R	Turn radius
$\dot{V}$	Acceleration along flight path, equivalent to a_X
W	Aircraft weight
X	Downrange distance
Y	Crossrange distance
α	Angle of attack
δ	Pitch control surface deflection
δ_A	Aileron deflection
Δ	Incremental difference
Θ	Aircraft pitch angle
λ	Thrust Vector angle
Φ	Bank angle
Ψ	Heading angle
$\dot{\Psi}$	Turn Rate

I. Introduction

Agility

Much of present fighter performance research centers on agility. Projects such as NASA's High Angle of Attack Research Vehicle (HARV)[1] and Rockwell/MBB's X-31 [2,3] represent current agility research. Interest from industry and NASA has created a host of analysis methods and agility philosophies.[4-7,13-17] Although several companies have developed their own measures of merit, the industry as a whole has not yet adopted a solid definition of agility nor accepted a particular agility metric or analysis method.

A sampling of the agility definitions used by industry include the inverse of the time to transition from one maneuver to another (Pierre Sprey [7]), the ability to rapidly change both the magnitude and direction of the aircraft velocity vector (Northrop [7]), the ability of the entire weapon system to minimize the time delays between target acquisition and target destruction (Eidetics [7]), and the capacity to change aircraft attitude and flight path with quickness and precision (Air Force Flight Test Center [8]),. Each of these definitions place emphasis on different facets of the concept of agility. It is the flight test maneuvers and their associated parameters that this paper discusses in detail.

In the final analysis, agility must provide a combat advantage over other aircraft--other factors such as training and weapons being equal. Historically, this has been created through improvements in energy maneuverability: the ability to generate high turn rates, speeds, and accelerations. However, performance of the lastest generation of fighters reaches and exceeds many physiological limits of the pilot, surpassing the g tolerance of humans and placing a limit on combat advantage through further improvements in energy maneuverability.

Given these human physiological barriers, trade studies performed at the preliminary design stage to enhance agility are thus vitally important. The purpose of this study is to demonstrate the inclusion of agility analysis based on flight test maneuvers that evaluate agility into the ACSYNT (AirCraft SYNThesis) design code developed at the NASA Ames Research Center. ACSYNT is a FORTRAN program currently used for preliminary design of aircraft. It is composed of modules that perform different analysis functions relevant to aircraft design.

ACSYNT Code

The primary modules in ACSYNT are the geometry, trajectory (mission profile), aerodynamics, propulsions, and weights modules. These are called separately and iteratively until they converge on a design configuration that can perform the specified mission under given constraints.

The real power of ACSYNT is achieved when it is linked to another NASA code called COPES. This code is a generic optimization code. When ACSYNT and COPES are coupled, multivariable optimizations can be performed to perform trade studies of configurations and to evaluate the impact of technologies on configurations. The improvements in materials, propulsions and other technologies can be incorporated and their effect on aircraft configurations readily determined.

The objective of the agility module in ACSYNT is to analyze agility criteria that are suitable for flight testing. This analysis is intended to provide insight into combat effectiveness early in the aircraft design phase. In the next section flight test maneuvers, such as combat cycle time, are analyzed as potential agility metrics. Then the preliminary design process is illustrated with combat cycle time as an agility constraint for optimization. Finally, some comments are offered for the utility of this technique relative to flight testing and suggestions are made for future investigations.

II. Agility Metrics and Maneuvers

The goal of ACSYNT's agility module is to simulate existing agility maneuvers and to analyze their associated agility metrics. It is also designed to accomodate and adapt to future metrics. The agility module simulates flight on the boundary of what is frequently referred to as the doghouse plot, a graph of turn rate versus speed or Mach number as shown in **Figure 1.** The upper boundary of this graph indicates the maximum turn rate for a given Mach number. There is a peak in the upper boundary representing the highest achievable turn rate, and the Mach number corresponding to this peak is called corner speed.

The aircraft is said to be "load limited" when its speed exceeds corner speed, with the maximum turn rate determined by the maximum designed load factor. Below corner speed, the aircraft is operating at its maximum lift coefficient and is said to be "lift limited." Corner speed produces the maximum design load factor at maximum lift coefficient.

Flight Test Maneuvers as Agility Metrics

Combat Cycle Time (CCT). Combat cycle time measures the time it takes to turn through a specified heading change and then accelerate to regain the energy lost during the turn. The objective is to complete this maneuver in the least amount of time. In this maneuver the aircraft operates along the boundary of the doghouse plot starting at maximum speed as shown in **Figure 1.**

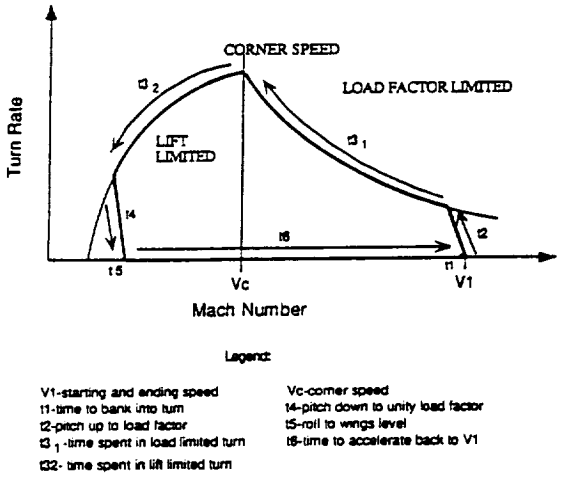

Figure 1. Doghouse Plot

Pointing Margin. The pointing margin metric measures how fast an aircraft can be pointed at an adversary aircraft. In a test maneuver to measure pointing margin, the two aircraft cross at nearly the same location in space at the same Mach but pointed in opposite directions (see **Figure 2**). Both aircraft begin a maximum acceleration turn toward one another. The aircraft that first brings his line of sight upon the opposing aircraft's position is considered the most agile. The measure of merit is the pointing margin or the angle between the two aircrafts' lines of sight just as the inferior aircraft is captured. The greater this angle the longer it takes the losing aircraft to acquire the winning aircraft's position. This provides the winning aircraft a longer missile flight time and a better chance of a kill.

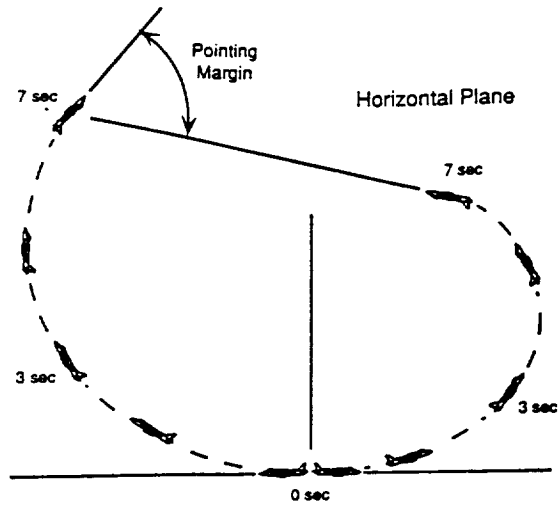

Figure 2. Pointing Margin Agility Maneuver

Torsional Agility [7] For a given altitude and Mach number, the maximum possible turn rate divided by the time to perform a 90 degree roll maneuver measures an aircraft's torsional agility, the ability to quickly rotate the acceleration vector about the longitudinal axis.

Axial agility [9] Axial agility measures the influence of the propulsion system on the aircraft's ability to quickly gain or lose energy. For a given altitude and Mach number, axial agility is the difference between maximum and minimum specific excess power divided by the time for the aircraft to transition between these two power levels, i.e.

$$\frac{Ps_{max} - Ps_{min}}{\Delta t}$$

For this metric both the transient time and the range of excess power levels are important.

Dynamic Speed Turn [5] The dynamic speed turn consists of a pair of graphs that relate two parameters over an entire flight envelope. The plots are maximum turn rate versus bleed rate and the maximum straight and level acceleration versus Mach number. These plots correspond to a given altitude. Two example dynamic speed turn plots are illustrated in **Figures 3 and 4.**

The bleed rate graph plots the maximum turn rate at full thrust for all possible Mach numbers versus the corresponding axial acceleration (bleed rate). The bleed rate and the maximum level acceleration curves illustrate how an aircraft loses energy during maneuvering and how fast it can gain energy after maneuvering.

The above flight test maneuvers and associated agility metrics analyze how efficiently aircraft use energy to achieve an objective and also how quickly they can regain lost energy. Combat cycle time is the metric chosen to be simulated in this work because it contains elements of many points of view. It not only focuses on the gain and loss of energy, but also contains quick-action maneuvers (roll and pitch) within it. The methodology used to develop the CCT agility module architecture is the subject of the next section.

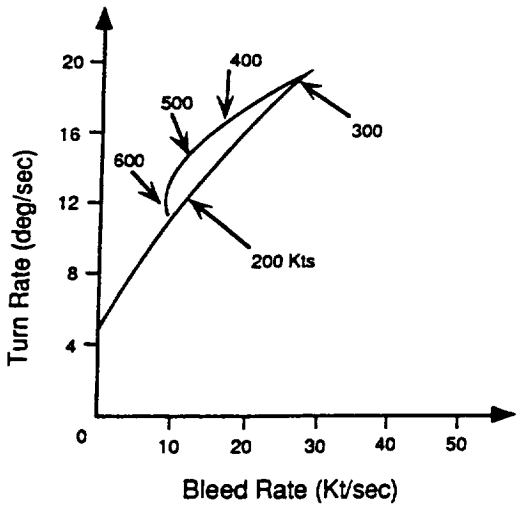

Figure 3. Turn Rate vs Bleed Rate in a Dynamic Speed Turn

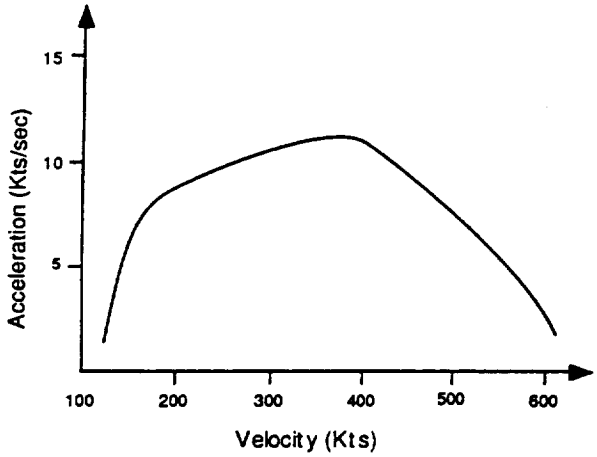

Figure 4. Level Acceleration in Dynamic Speed Turn

III. Integrating Agility into ACSYNT

General Methodology.

The design and analysis design code presented here tracks pertinent agility parameters (such as Mach number and turn rate) over the course of an agility maneuver. Each agility subroutine is basically a time stepping simulation of the associated flight test technique. To evaluate agility metrics other than combat cycle time, one of two options may be used. The user may input the desired maneuver segments into an existing agility subroutine or may create a different agility subroutine with different maneuver segments and parameters

Constant Altitude Assumption. A constant altitude assumption is made to simplify the resulting equations; however, the aircraft simulation is not constrained to fly level. The vertical excursions are simply ignored in the analysis. It is the user's responsibility to ensure maneuvers are substantially level during the simulation.

Maneuver Segments. The agility maneuvers were divided into separate segments. Figure 5 illustrates the four types of maneuver segments: rolls, pitches, turns, and accelerations. Segments are further divided into functional and transient categories. Functional maneuver segments deal with long-term changes in aircraft energy state, position and attitude. Equations of motion for the functional segments were steady-state equations for turns and rectilinear flight. Transient maneuver segments deal with short-term changes in aircraft accelerations, positions and orientation. Equations of motion for the transient segments were standard longitudinal and lateral-directional perturbation equations.

Quasi-Steady Maneuvers. Turns and accelerations actually represent quasi-steady turns and straight line accelerations. The term "quasi-steady turn" refers to a steady, level turn maneuver where the velocity may be changing. If a turn cannot be sustained the aircraft loses airspeed. In order to maintain the load factor, the angle of attack must gradually increase. If the aircraft is lift-limited and cannot sustain the load factor, the bank angle must gradually decrease to maintain the level turn. These changes in angle of attack and bank angle occur slowly so that the steady turn equations of motion can be used and the perturbation equations need not be employed. It is this type of turning maneuver that is termed quasi-steady.

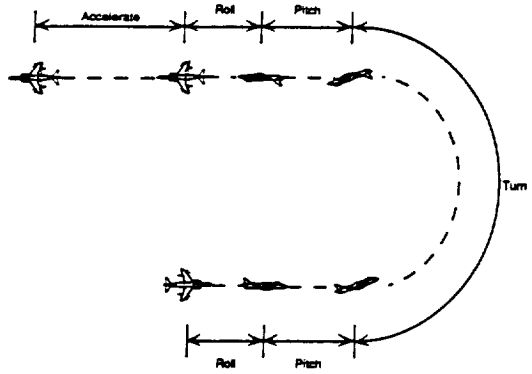

Figure 5. Agility Maneuver Segments

Tracked Variables

In order to evaluate agility metrics, nineteen parameters must be tracked. For each time step these parameters are calculated and stored. The primary output of the agility module is a time-stepped array of these parameters. The nineteen tracked variables are listed in Table 1.

A few of the parameters may need explanation. Axial acceleration is the acceleration along the velocity vector. The thrust vector angle parameter is pilot commanded. It does not represent pitch control thrust-vectoring but thrust vector rotation about the aircraft center of gravity as in powered-lift aircraft such as the McDonnell Douglas AV-8B. Net thrust is gross thrust minus the momentum flux at the inlet (ram drag). At zero airspeed gross and net thrust are identical. As airspeed increases ram drag increases and the net thrust developed by the engine decreases. These two parameters are important during thrust-vectoring maneuvers. It is the gross thrust that is vectored normal to the flightpath. The ram drag (Tg-Tn) however, remains in the airflow (axial) direction. The engine core percent and afterburner percent represent the core thrust over full dry thrust and the afterburner thrust over full afterburner thrust respectively.

Table 1. Variables Tracked Over Time by the Agility Module

M mach number	V axial acceleration (g's)	Throttle command logic (numeric)	λ thrust vector angle (degrees)
Tg gross thrust (pounds)	Tn net thrust (pounds)	Engine core thrust (% thrust)	Afterburner thrust (% thrust)
α angle of attack (degrees)	n normal accel. 'load factor' (g's)	C_L lift coefficient	C_D drag coefficient
γ heading angle (degrees)	ψ turn rate (deg/sec)	Φ bank angle (degrees)	p roll rate (deg/sec)
X downrange distance (feet)	Y crossrange distance (feet)	R turn radius (feet)	

Reference Frames.

The functional maneuver strategy uses steady state maneuver equations, and the transient maneuver strategy uses lateral and longitudinal perturbation equations of motion for the roll and pitch segments[10]. Appropriate coordinate systems are developed to implement these strategies.

The inertial, earth-fixed system is designated (X1, Y1, Z1) and is used to measure downrange and crossrange parameters (X,Y) as shown in **Figure 6.** The second coordinate system (X2, Y2, Z2) translates with the aircraft but does not rotate with it, and a third coordinate system (X3, Y3, Z3) rotates in heading (the angle between the X2 axis and the X3 axis) and roll (the vertically projected angle between the X2-Y2 plane and the Y3 axis). Since the aircraft is constrained in altitude the velocity vector (and hence X3) must always lie in the X1-Y1 plane. At time zero all three coordinate systems coincide with their origins at the aircraft center of gravity.

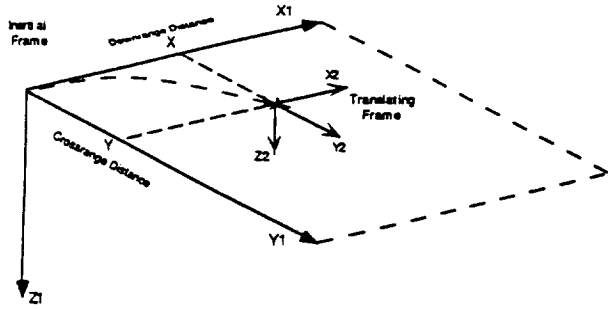

Figure 6. Reference Frames

Basic Equations for Functional Segments.

Figure 7 illustrates the free-body diagram used to determine the parallel (axial) acceleration component. From this diagram

$$T_g \cos(\alpha+\lambda) - D_{aero} - D_{ram} = \left(\frac{W}{g}\right) a_x \qquad (1)$$

Substituting for D_{aero} and D_{ram} and solving for a_X:

$$a_x = g\left[\left(\frac{T_g}{W}\right)\cos(\alpha+\lambda) - \frac{qC_D}{\frac{W}{S}} - \frac{T_g - T_n}{W}\right] \qquad (2)$$

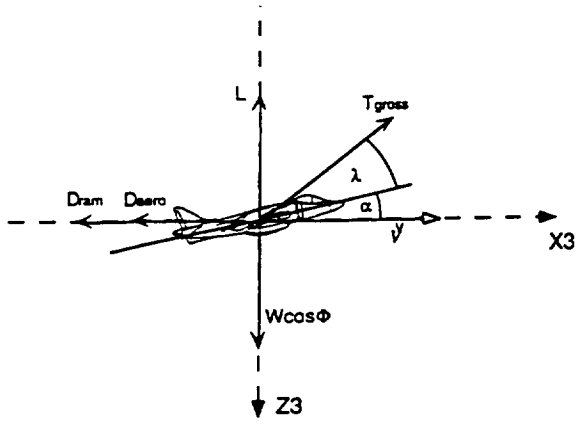

Figure 7. Aircraft Free Body Diagram for Longitudinal Acceleration

The free body diagram in **Figure 8** illustrates the forces that generate the normal acceleration component. For equilibrium in a steady level turn the aerodynamic and thrust acceleration element (a_F) must be balanced by the gravitational (g) and the centripetal (a_{cent}) elements. Thus

$$a_F^2 = a_{cent}^2 + g^2 \qquad (3)$$

The a_F element is represented by

$$\Sigma F_F = m a_F \qquad (4)$$

$$-T_g \sin(\alpha+\lambda) - L = \left(\frac{W}{g}\right) a_F \qquad (5)$$

Substituting for lift L and solving for a_F

$$a_F = g\left[\frac{-T_g}{W}\sin(\alpha+\lambda) - \frac{qC_L}{\frac{W}{S}}\right] \qquad (6)$$

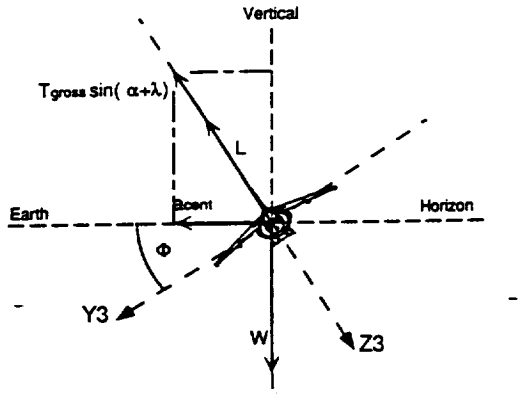

Figure 8. Aircraft Free Body Diagram for Normal Acceleration Component

Substituting a_F above yields

$$a_{cent} = g\left\{\left[\frac{T_g}{W}\sin(\alpha+\lambda)+\frac{qC_L}{\frac{W}{S}}\right]^2 - 1\right\}^{\frac{1}{2}} \quad (7)$$

Equations for the turn radius and turn rate can be determined from basic rotational kinematics. The relationship between turn radius, velocity and centripetal acceleration is

$$R = \frac{V^2}{a_{cent}} \quad (8)$$

Substituting into a_{cent} results in

$$R = \frac{V^2}{g\left\{\left[\frac{T_g}{W}\sin(\alpha+\lambda)+\frac{qC_L}{\frac{W}{S}}\right]^2 - 1\right\}^{\frac{1}{2}}} \quad (9)$$

Substituting the arc length $s = R\Psi$ of a curved flight path and its derivative $V = R\dot{\Psi}$ results in

$$\dot{\Psi} = \frac{g\left\{\left[\frac{T_g}{W}\sin(\alpha+\lambda)+\frac{qC_L}{\frac{W}{S}}\right]^2 - 1\right\}^{\frac{1}{2}}}{V} \quad (10)$$

Basic Equations for Transient Segments.

Equations of motion for the transient segments are the standard lateral-directional and longitudinal perturbation equations of motion. From these equations standard approximations are made to achieve simplified modal responses.

Roll Segments. The roll segments were modeled with a single degree of freedom, lateral equation of motion as given in Reference 10. The basic equation relating the roll damping derivative (L_p), aileron effectiveness derivative ($L_{\delta a}$), and aileron deflection (δa) is:

$$\dot{p} = L_p p + L_{\delta a}\delta_a \quad (11)$$

Note: ACSYNT will not provide dimensional derivatives L_p and $L_{\delta a}$. They are input directly by the user.

Figure 9 illustrates a typical roll maneuver as simulated by the code. As the roll progresses following a step aileron deflection the control input is reversed. This creates a strong roll deceleration. If this control reversal is timed properly (an iterative technique is required), the roll rate drops to zero just as the target bank angle is acquired. This control strategy provides the quickest roll maneuver possible for a given aileron deflection. The roll rate and bank angle schedules were calculated by integration of the roll equation with the proper initial conditions.

The bank angle during initial control input is

$$\Phi(t) = \Phi_0 + p_{ss}\left(t + \frac{1}{L_p}\left(1 - e^{L_p t}\right)\right) \quad (12)$$

The bank angle after the control reversal is:

$$\Phi(t) = \Phi_0 + \frac{p_{ss}}{L_p}\left(2e^{L_p(t-t^*)} - e^{L_p t} - 1\right) - p_{ss}\left(t - 2t^*\right) \quad (13)$$

where t* is the time of the control input reversal.

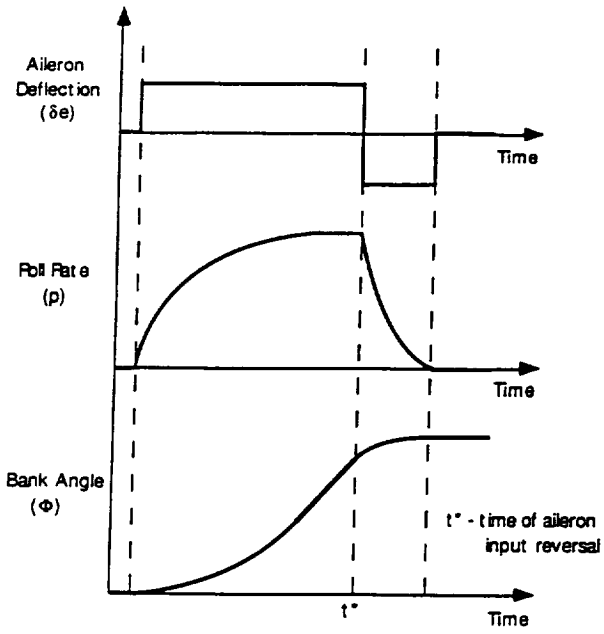

Figure 9. Roll Maneuver

Pitch Segments. The pitch equations of motion were the standard two degree of freedom short-period approximation equations of mtoion as developed in Reference 10. The s-domain (LaPlace) matrix form is

$$\begin{bmatrix} sU_1 - Z_\alpha & -U_1 s \\ -\{M_{\dot\alpha}s + M_\alpha\} & s^2 - M_q s \end{bmatrix}\begin{Bmatrix} \frac{\alpha(s)}{\delta(s)} \\ \frac{\Theta(s)}{\delta(s)} \end{Bmatrix} = \begin{Bmatrix} Z_\delta \\ M_\delta \end{Bmatrix} \quad (14)$$

The dimensional derivatives for the above matrix were input by the user since ACSYNT will not calculate stability or control derivatives.

A typical pitch time response is shown in **Figure 10** for a step control deflection. The angle of attack starts at zero and ends at the steady state angle of attack corresponding to the new control deflection. The pitch model thus consists of a transient angle of attack time response due to a step control input. The load factor resulting from this control input is the steady state load factor due to the instantaneous angle of attack. This strategy provides a satisfactory pitch transient with the least complicated and fastest execution time.

Aircraft configurations were constrained to a pitch damping ratio of at least 0.7 to avoid numerical problems in the integration routine. If the configuration did not have this level of damping the derivatives Cm_q and $Cm_{\dot\alpha}$ were artificially increased to provide sufficient damping. This constraint approximates the effects of a flight control system that limits pitch overshoot. Unstable configurations were also artificially constrained to prevent numerical instabilities in the pitch equations. The pitching moment slope Cm_α was forced to be -0.1 or less. This method places a warning flag

in the output file. Fortunately, transient segments contribute little to the overall maneuver performance and so these simplifications did not seriously affect the results. However, totally accurate analysis for unstable aircraft will only be possible when ACSYNT's planned Flight Dynamics Module is introduced.

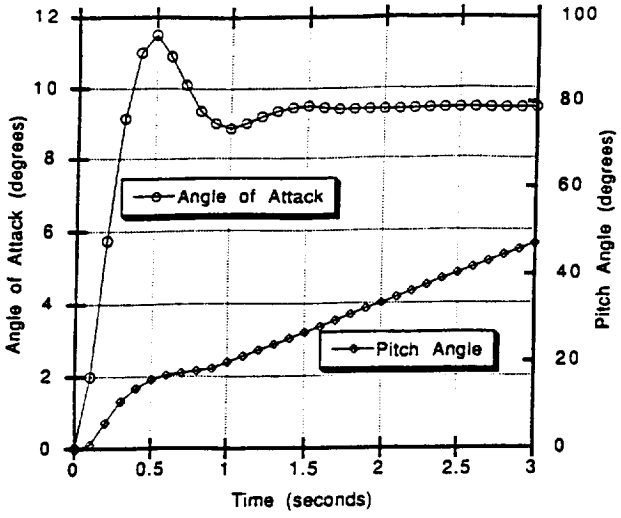

Figure 10. Typical Pitch Response to Step Elevator Deflection

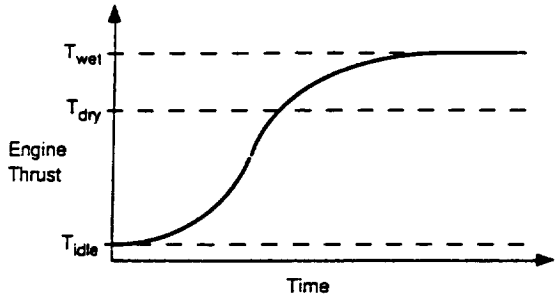

Figure 11. Throttle Transient Response from Flight Idle to Max Afterburner

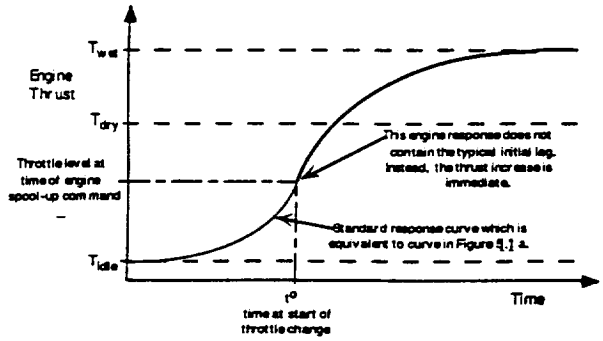

Figure 12. Throttle Transient Response from Partial Dry to Max Afterburner

Thrust Segments. The engine transient model was based on non dimensional data for a 1990s era low-by-pass turbofan fighter engine. This data consisted of six particular throttle responses listed in **Table 2**.

Table 2. Throttle Response Time Histories

Max afterburner -> Flight idle	Max afterburner -> Max dry
Max dry -> Flight idle	Flight idle -> Max dry
Flight idle -> Max afterburner	Max dry -> Max afterburner

Figure 11 shows the time histories of one of these six throttle responses. At any time step, the commanded thrust level may be changed by code logic. When this occurs the proper throttle response curve is enacted to provide a time history of the engine transient. The remaining responses may be found in Reference 18.

Throttle changes do not always fit one of the six throttle responses. In this case, the code begins its time history in the middle of the appropriate response curve. **Figure 12** illustrates an example of this technique. The main drawback to this method is that, instead of an initial lag, the power increases rapidly from the beginning of the throttle change.

Code Options and Features

Angle of Attack Limiting. The user has control of the maximum angle of attack, thus providing a reference for determining maximum lift coefficient. ACSYNT's aerodynamic module does not calculate a discrete stall angle of attack. Without an obvious stall point, the definition of maximum lift coefficient is difficult to pinpoint; therefore, the angle of attack limiter is a necessary input.

Definition of Turning Speed. The simulation package is set up to maintain a desired airspeed, determined by the code, called turning speed. Turning speed is the Mach number corresponding to the intersection of the lift-limit curve and the load-limit curve of the doghouse plot in **Figure 1** when the load-limit curve does not correspond to the maximum design load factor. This logic is incorporated to keep the maneuvering aircraft in the most favorable Mach number regime for high turn rates.

There are two ways that the code specifies turning speed depending on user input. The load factor for turning speed may be selected as a variable by the user for the turn maneuver. **Figure 13** shows various turning speeds as determined by user-selected load factors for the same aircraft. The second way that turning speed may be selected is by direct Mach number input. Allowing the user to set the turning speed may result in better overall simulated maneuver performance when time to accelerate is included.

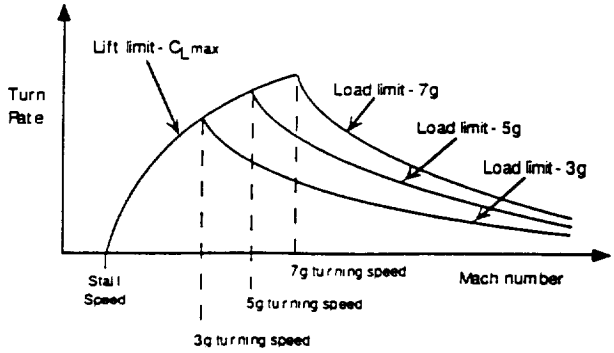

Figure 13. Variation of Turning Speed with Turning Load Factor

Throttle Control and Turning Speed Capture

The simulation package maintains turning speed through throttle manipulation. In order to achieve this the user inputs throttle settings. There are two throttle settings for each maneuver segment: one for airspeeds above turning speed and the other for airspeeds below turning speed. By commanding a low power level above turning speed, the aircraft can be decelerated to turning speed. Conversely, high power level below turning speed can accelerate the aircraft to turning speed.

Mach number LEAD. Another input parameter, MLEAD, can be used to alter the throttle command technique to provide a buffer zone around the turning speed. It causes the code to change throttle settings before the turning speed is achieved. It simulates pilot anticipation of turning speed by leading the throttle change. **Figure 14** shows how the parameter MLEAD affects the throttle command schedule. If the turn is not sustainable then the thrust is set at the maximum afterburning setting.

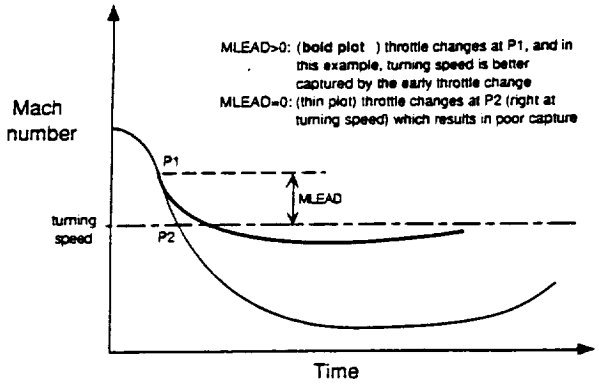

Figure 14. Throttle Control Logic with MLEAD Parameter

Thrust Vectoring. The thrust vectoring capability of the agility module is not conventional pitch control thrust-vectoring but the ability to rotate the thrust vector about the center of gravity as in the direct-lift capability of aircraft such as the Hawker Siddeley Harrier and McDonnell Douglas AV-8B. It allows the aircraft to generate some of the turning load factor with thrust normal to the flight path resulting in higher turn rates for a given aerodynamic load factor; however, this reduces the axial component of thrust.

The thrust vector angle (λ) is the angle between the fuselage axis and the thrust vector controlled by the user during each maneuver segment. The angle can range from zero to 180 degrees. The transition rate ($\dot{\lambda}$) is also a user input. Each segment has two vector inputs for operation above and below turning speed. This allows the user to better model a pilot's control technique in maintaining the aircraft's turning speed.

Airbrake The user has the option of employing an airbrake during metric maneuvers by providing an equivalent flat plate area for the extended airbrake. This drag is included with the aircraft's clean drag. Once the airbrake option is selected, the control and operation of the airbrake is automatic. The airbrake is automatically extended when the aircraft is flying above turning speed and, conversely, the airbrake is automatically retracted when the aircraft is below turning speed. The retraction sequence was assumed to be instantaneous over one time-step.

External Stores,Weight, Moment of Inertia.

The user specifies the desired percent fuel load including the internal and any external fuel the aircraft may be carrying. The weight and drag of these stores is specified in the weight and aerodynamic input files of ACSYNT. The moment of inertia for the aircraft with pylons, as well as the incremental moments of inertia for fuel and stores, is specified in the agility input file. During any maneuver segment the agility module has the capability of dropping stores by nulling the store's weight and moments of inertia. Each segment contains logical drop flags for four types of stores: missiles, bombs, external fuel tanks, and ammunition. When the user inputs the dimensional derivatives for the roll maneuver segment they must be referenced to a moment of inertia. The roll response is thus dependent on the aircraft fuel and stores loading.

Agility Code Verification

The agility subroutine was verified in two phases.[18] The first phase tested code logic to ensure continuous and reasonable time histories of the tracked variables. The angle of attack limiter, airbrake, turning speed capture and thrust-transient model all performed as designed and the integrity of the coding technique was considered satisfactory.

The second phase compared the agility module's maneuver analysis with the combat analysis capability already contained in ACSYNT's trajectory module. This phase ensured that the agility module was retrieving aerodynamic and propulsive data properly and that the results were consistent with an independent performance package NASA has used for years. The results, documented completely in Reference 18, showed agreement within three percent for all tracked variables. Note that the combat analysis already within the ACSYNT module conducts its analysis at a frozen instant in time. The agility module performs these calculations for consecutive time steps and calculates the resulting kinematics between these time steps. The verification procedures indicated that the agility module performs time dependent maneuverability analysis properly. This procedure also indicates that the time-stepping simulation package is an effective method of tracking an aircraft's performance throughout a manuever.

IV. Case Studies

In this chapter the influence of two parameters, thrust loading and wing loading, on the combat cycle time metric are investigated. In Reference 18 an additional example using the COPES optimization code in conjunction with ACSYNT is accomplished to optimize the wing loading and thrust loading for minimum gross takeoff weight. These studies are intended to illustrate how the agility module may be used to ascertain and optimize an aircraft configuration's agility potential. The agility metric analysis will show that aircraft having similar energy maneuverability performance can have substantially different levels of agility as evaluated by the simulation of agility flight test metrics.

The baseline aircraft used for the studies was a fighter aircraft similar to a Northrop F-20 Tigershark. The weights, external dimensions and installed thrust were matched to obtain a representative fighter model. The maneuver used for this metric was a 7g turn through 180 degrees at an altitude of 15,000 feet. The aircraft began the maneuver in straight and level flight at Mach 0.9.

Effect of Thrust Loading on Combat Cycle Time

The Combat Cycle Time (CCT) maneuver was performed using the baseline fighter configuration. For comparison, four other configurations were flown, altered only in the available level of thrust (80%, 90%, 110%, and 120%). The full power thrust loading of the baseline configuration was 0.94. For the 80% and 120% thrust aircraft this corresponded to thrust loadings of 0.75 and 1.13 respectively.

Although only the thrust level was changed and all other input parameters were held constant, convergence of each aircraft during ACSYNT execution resulted in slight variation in aircraft weight. This resulted in a maximum difference in wing loading of 78.3 for the 80% thrust configuration and 78.5 for the 120% configuration.

Figure 15 illustrates the time differences for each segment of the CCT maneuver for all five configurations. As would be expected, the highest thrust aircraft performed the maneuver in the least amount of time. The maneuver times also steadily decreased with increased available thrust. This is because the reduced velocity deficit coupled with the more powerful engine created significantly shorter acceleration times for the higher thrust configurations.

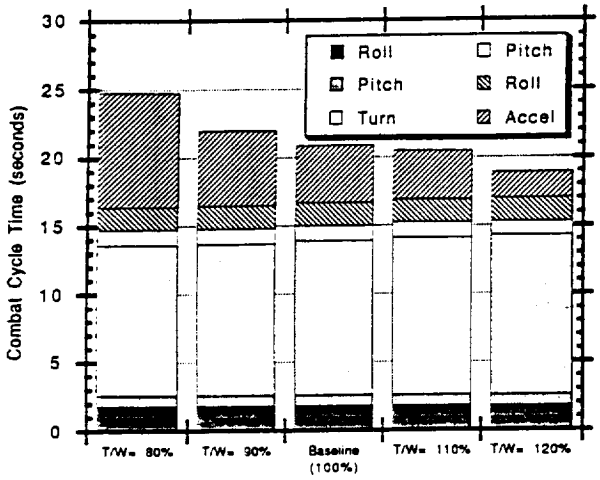

Figure 15. CCT Variation with Thrust Load

The turning performance is evident in **Figure 16.** Only the 80% thrust configuration achieves turning speed. The lower thrust configurations turn tighter and possess a positional advantage over the course of the turn segment. However, as the aircraft accelerate back to the starting velocity the lower thrust aircraft take longer and by the time the maneuver is completed they have lost their positional advantage. For time considerations the higher thrust aircraft appeared to win across the board. For longer turns of 360 degrees, the lower thrust aircraft would most certainly lose.

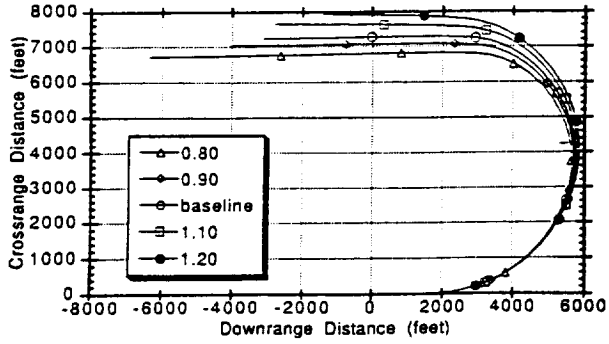

Figure 16. Turn Diagrams for Different Engine Thrust Loading

Effect of Wing Loading on Combat Cycle Time

Combat Cycle Time maneuvers were performed using four different wing loadings for comparison with the baseline configuration. The selected wing loadings were 65, 70, 85, and 90 pounds per square foot (baseline 78.4 psf). However, convergence of the aircraft during ACSYNT execution resulted in weight disparity and a consequent difference in thrust loading for the five configurations. The extremes were a thrust loading of 0.96 for the 65 psf wing loading configuration and 1.00 for the 90 psf configuration.

Figure 17 illustrates the time differences for each segment of the Combat Cycle Time maneuver for all five configurations. The total time to complete the maneuver was very similar for all configurations. There was, however, a difference in the times for each maneuver segment. **Figure 18** plots the turn profile in the horizontal plane of the maneuver. The aircraft with higher wing loading has both a time and a spatial turn advantage. By the time the entire maneuver was completed and the aircraft had re-accelerated to the starting velocity all five configurations flew roughly abreast of one another.

Note that the turning speed depends on wing loading and so is different for each configuration. As the wing loading decreases the turning speed decreases as well. The 65 psf aircraft never reaches its turning speed through the 180 degree turn. If the turn were extended to 270 or 360 degrees the aircraft with higher wing loading would have lost its turning advantage and created an excessive velocity deficit that would lengthen the acceleration phase. This shows the difficulty in developing robust agility criteria that provide the best overall performance for a variety of situations and tasks.

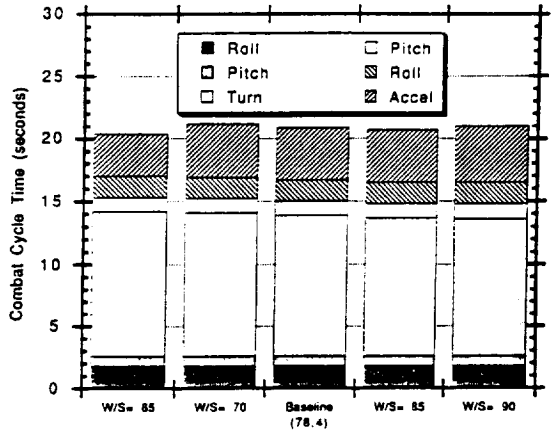

Figure 17. CCT Variation with Wing Load

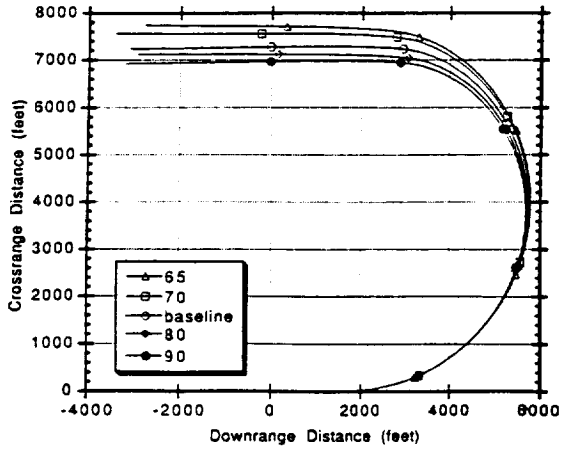

Figure 18. Turn Diagrams at Different Wing Loading

Use of CCT as a Constraint In Aircraft Design Optimization

This section illustrates how the agility module can be used in configuration optimization. This capability is the real power of ACSYNT and it is these types of optimization studies that can be used to determine the impact of agility technologies and constraints on the overall aircraft configuration. The overall optimization technique will first be discussed and then the particular example will be presented to illustrate the optimization opportunities of the agility module.

The basic optimization method used by COPES in conjunction with ACSYNT consists of an objective variable, design variables and constraint variables. The objective variable is the parameter that is being optimized and can be either maximized or minimized. Design variables are the parameters whose values are varied to provide a design space. These design variables are given upper and lower bounds. The constraint variables are parameters that further limit the design space. In the case of ACSYNT typical constraints are mission range or a sustained turn requirement at altitude. Only the design variable space that satisfies all constraints can provide possible solutions. The optimizer evaluates aircraft configurations over this design space and attempts to find the design point that produces the desired extrema of the objective variable.

In this example the objective variable is gross takeoff weight. The constraint for this optimization is to complete the same CCT maneuver used previously within 20.00 seconds. The design variables are the wing area and engine size. **Table 3** lists the design variables bounds, the constraint variable value, and the pertinent parameters of the starting configuration and the optimized configuration. This information is also illustrated in **Figure 19**.

The tradeoff in this case is wing loading versus thrust loading. A decrease in wing loading allows a decrease in thrust loading and vice versa. However, a larger wing adds weight to the vehicle. Conversely a larger engine also adds weight. These two trends are the source of the tradeoff that drive the wing to as small a value as possible. This results in only a moderate increase in engine size. Evidently the agility criterion is much more sensitive to engine size than wing loading.

The lower boundary on wing loading can be reduced to see where the wing size stabilizes. The wing continues to shrink to 90 square feet, an unreasonable result caused by using CCT as the only constraint. Any functional aircraft configuration would have many more constraints that would require a reasonable wing size. This example does show, however, the capability of ACSYNT to use agility constraints in configuration optimization.

Table 3. CCT Optimization Results

Design and Constraint Variable Boundaries		
Design variable	Lower bound	Upper bound
Wing area (ft^2)	150.0	250.0
Engine scale factor	0.200	1.00
Constraint variable	**Lower bound**	**Upper bound**
Combat Cycle Time (sec.)	5.00	20.0

Optimization Results		
Configuration:	Original	Optimized
Combat Cycle Time (sec.)	21.40	20.00
Wing area	200.0	150.0
Engine scale factor	0.420	0.438
Takeoff weight	19,234	18,904

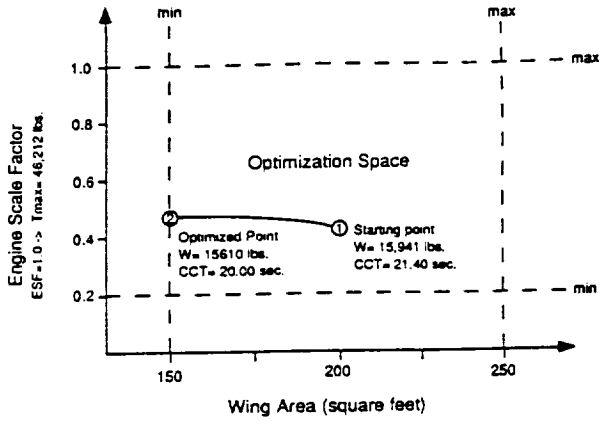

Figure 19. CCT Design Optimization Results

V. Conclusions and Recommendations

This paper presents the overall architecture of an agility module that is an effective tool in analyzing an aircraft configuration's agility potential. The example studies of the effect of thrust loading and wing loading illustrate how the module can be used to perform trade studies on parameters important to agility metrics that are based on flight test maneuvers.

The module is also capable of providing constraints for ACSYNT's optimization capability. Once agility criteria have been developed the module can be used to optimize an aircraft configuration for agility requirements as well as contemporary mission requirements. It is particularly suited to metrics such as combat cycle time, pointing margin, and dynamic speed turn.

The agility module's architecture has an important characteristic for future improvements. Since industry has not yet settled on a single definition of agility, the adaptable architecture will allow future metrics and requirements to be incorporated.

Ongoing work at Nasa Ames is continuing the investigation of the Combat Cycle Time agility maneuver and includes a design study which will use existing flight data of agile maneuvers to validate the simulation and its underlying assumptions. The existing simulation module will be enhanced by including stability and control derivatives and by implementing a more friendly user interface. Future work will include development of a computer simulation and design optimization module for the pointing margin agility maneuver.

Acknowledgment

The authors are grateful to Mr. Andrew Hahn, Mr. Jeffrey Samuels, Mr. Paul Gelhausen and Mr. George Kidwell at NASA Ames for their guidance and support.

References

[1] Gilbert, W. P., et al. "Control Research in the NASA High-Alpha Technology Program." AGARD Conference Proceedings AGARD-CP-465. Symposium of the Fluid Dynamics Panel. Madrid, Spain. October 2-5, 1989.

[2] Wanstall, B., and J.R. Wilson. "Air Combat Beyond The Stall." Interavia Aerospace Review, Vol. 45, May 1990, 405-407.

[3] Herbst, W. B. (MBB). "X-31A." SAE Paper 871346. SAE Aerospace Vehicle Conference. Washington, DC. June 8-10, 1987.

[4] Dorn, M. "Aircraft Agility: The Science and the Opportunities." AIAA Paper AIAA-89-2015. AIAA/AHS/ASEE Aircraft Design, Systems and Operations Conference. Seattle, Washington. July 31 - August 2, 1989.

[5] McAtee, T. "Agility in Demand." Aerospace America, May 1988, 36-38.

[6] Tamrat, B.F. "Fighter Aircraft Agility Assessment Concepts and Their Implication on Future Agile Fighter Aircraft." AIAA Paper AIAA-88-4400. AIAA/AHS/ASEE Aircraft Design, Systems and Operations Meeting. Atlanta, Georgia. September 7-9 1988.

[7] Skow, A.M. "Agility As a Contribution to Design Balance." AIAA Paper AIAA-90-1305. AIAA/SFTE/DGLR/SETP Fifth Biannual Flight Test Conference. Ontario, California. May 1990.

[8] Butts, S., and A. Lawless. "Flight Testing for Aircraft Agility." AIAA Paper AIAA-90-1308. AIAA/SFTE/DGLR/SETP Fifth Biannual Flight Test Conference. Ontario, California. May 1990.

[9] Liefer, R. K., et al. "Assessment of Proposed Fighter Agility Metrics." AIAA Paper AIAA-90-2807. AIAA Atmospheric Flight Mechanics Conference. Portland, Oregon. August 20-22, 1990.

[10] Roskam, J. Airplane Flight Dynamics and Automatic Flight Controls Part 1. Lawrence, Kansas: Roskam Aviation and Engineering Corporation, 1982.

[11] Roskam, J. Airplane Design Part VI: Preliminary Calculation of Aerodynamic, Thrust and Power Characteristics. Lawrence, Kansas: Roskam Aviation and Engineering Corporation, 1987.

[12] McRuer, D., and I. Ashkenas. Aircraft Dynamic and Automatic Control. Princeton, University Press, 1973.

[13] Bitten, R. "Qualitative and Quantitative Comparison of Government and Industry Agility Metrics." AIAA Paper AIAA 89-3389. AIAA Atmospheric Flight Mechanics Conference. Boston, Massachusetts. August 14-16, 1989.

[14] Skow, A.M., et al. "Advanced Fighter Agility Metrics." AIAA Paper AIAA 85-1779. AIAA Atmospheric Flight Mechanics Conference. Snowmass, Colorado. August 18-21, 1985.

[15] Yajnik, K. S. "Energy-Turn-Rate Characteristics and Turn Performance of an Aircraft." Journal of Aircraft, Vol. 14, May 1977, 428-433.

[16] Riley, D., and M. Drajeske. "Status of Agility Research at McDonnell Aircraft Company and Major Findings and Conclusions to Date." ICAS Paper ICAS-90-5.9.4. ICAS, Congress, 17th. Stockholm, Sweden. September 9-14, 1990.

[17] Riley, D., and M. Drajeske. "An Experimental Investigation of Torsional Agility in Air-to-Air Combat." AIAA Paper AIAA 89-3388. AIAA Atmospheric Flight Mechanics Conference. Boston, Massachusetts. August 14-16, 1989.

[18] Bauer, B.A., "Development of A Computer Program for Analyzing Preliminary Aircraft Configurations in Relationship to Emerging Agility Metrics," Masters Thesis, Cal Poly State University, December 1993.